High-spectral-resolution coherent anti-Stokes Raman scattering with interferometrically detected broadband chirped pulses

Gareth W. Jones, Daniel L. Marks, Claudio Vinegoni, and Stephen A. Boppart

Biophotonics Imaging Laboratory, Beckman Institute for Advanced Science and Technology, Department of Electrical and Computer Engineering, University of Illinois at Urbana—Champaign, 405 North Mathews, Urbana, Illinois 61801

Received January 9, 2006; revised February 17, 2006; accepted February 22, 2006; posted February 22, 2006 (Doc. ID 67111)

To achieve high-spectral-resolution multiplex coherent anti-Stokes Raman scattering (CARS), one typically uses a narrowband pump pulse and a broadband Stokes pulse. This is to ensure a correspondence between anti-Stokes and vibrational frequencies. We obtain high-resolution CARS spectra of isopropanol, using a broadband chirped pump pulse and a broadband Stokes pulse, by detecting the anti-Stokes pulse with spectral interferometry. With the temporally resolved anti-Stokes signal, we can remove the chirp of the anti-Stokes pulse and restore high spectral resolution while also rejecting nonresonant scattering. © 2006 Optical Society of America

OCIS codes: 300.6450, 190.7110.

Coherent anti-Stokes Raman scattering (CARS), a spectroscopic tool for determining the vibrational frequencies of molecules, is finding an increasing role in biomedical imaging.[1,2] At the expense of more-complicated instrumentation, CARS provides a larger signal than spontaneous Raman scattering spectroscopy. In particular, CARS typically requires synchronized pump and Stokes pulses, which are obtained from a pair of synchronized lasers, or a pump and an optical parametric oscillator or amplifier. For multiplex CARS,[3,4] in which multiple vibrational frequencies are probed simultaneously, the pump pulse has a narrow bandwidth and the Stokes pulse has a broad bandwidth. A narrow pump pulse is needed to ensure that there is a pairwise correspondence between vibrational frequencies and anti-Stokes frequencies. Recently we proposed a method of multiplex CARS spectroscopy that uses chirped broadband pump and Stokes pulses.[5] Ultimately, a multiplex CARS instrument could employ a single femtosecond laser and pulse shaping apparatus, which one could easily reconfigure to probe many molecular resonances without retuning the laser. Multiplex CARS has been performed with chirped pulses without interferometric detection,[6] and multiplex CARS with chirped Stokes pulses[7] has also been explored. In addition, interferometric multiplex CARS has been performed,[8] but, to further our goal, we demonstrate, for the first time to our knowledge, the interferometric demodulation of high-resolution CARS spectra, using broadband pump and Stokes pulses.

Standard multiplex CARS utilizes a narrowband, transform-limited pump pulse and a broadband Stokes pulse that is coincident with the leading edge of the pump pulse. This situation is illustrated in Fig. 1(a). Assuming that only one vibrational resonance is excited, the anti-Stokes signal resembles a decaying sinusoidal oscillation. The power spectrum of this signal is the Lorentzian line shape. When an unchirped pump pulse is used, with its frequency increasing with time, as shown in Fig. 1(b), the anti-Stokes signal still resembles a decaying sinusoid. However, the anti-Stokes signal is now chirped identically to the pump pulse. The power spectrum of the anti-Stokes signal is no longer Lorentzian. Because a single vibrational frequency produces multiple frequencies in the anti-Stokes signal, we have lost the correspondence between vibrational and anti-Stokes frequencies. When multiple vibrations are excited, they produce overlapping and interfering spectra. Therefore, in general, the power spectrum alone may be insufficient to permit the Raman spectrum to be deduced, as it is in standard multiplex CARS.

If instead of measuring just the power spectrum of the anti-Stokes signal we measure the cross correlation of the anti-Stokes signal with a known reference signal, using an interferometric method such as spectral interferometry,[9] we can time resolve the anti-Stokes signal. Because all the polarizations produced by each vibrational mode mix with the same pump pulse, they all produce anti-Stokes signals that are chirped identically. By measuring the time-resolved

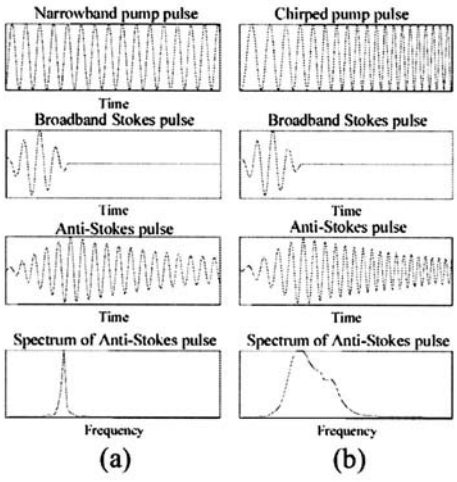

Fig. 1. Illustration of multiplex CARS with (a) a narrowband pump pulse and (b) a chirped broadband pump pulse.

0146-9592/06/101543-3/$15.00

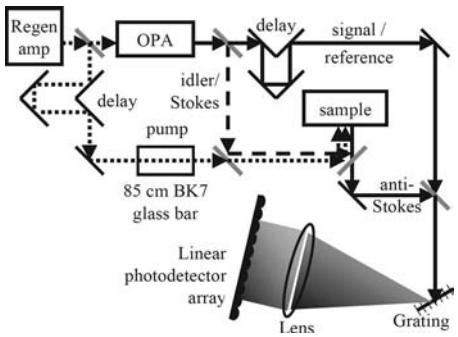

Fig. 2. Schematic of the optical system.

anti-Stokes signal, we computationally remove the chirp of the signal by multiplying the measured signal by the opposite chirp in the time domain. In doing so, we calculate the anti-Stokes signal that one would have measured if a narrowband pump pulse were used. Because the correspondence between vibrational frequencies and anti-Stokes frequencies is restored, one can determine the Raman spectrum from the corrected anti-Stokes spectrum. An additional benefit is that the complex Raman spectrum is obtained, with the imaginary part corresponding to the resonant Raman spectrum, so that nonresonant components can be discriminated.[8,10]

To explain the mathematics of chirped pump pulse CARS, we consider a chirped pump pulse with spectrum $\tilde{E}_p(\omega)=\tilde{E}_0(\omega)\exp[-i(\omega-\omega_0)^2/2\alpha]$, with $\tilde{E}_0{}^2$ being the power spectrum of the pump and α being the chirp rate of the pulse. Using the stationary phase approximation[11] yields, for a small α, the time-domain signal $E_p(t)=\alpha^{-1/2}\tilde{E}_0(\alpha t+\omega_0)\exp[i(\alpha t/2+\omega_0)t]$. The Stokes pulse spectrum $\tilde{E}_s(\omega)$ is transform limited and centered about $t=0$ such that $\mathrm{Im}[\tilde{E}_s(\omega)]=0$. Because of this, the instantaneous frequency of the pump pulse at the time the Stokes pulse arrives ($t=0$) is ω_0. If the Raman susceptibility of a sample being probed is $\tilde{\chi}^{(3)}(\Omega)$, where Ω is the vibrational frequency, Raman polarization $P^{(3)}(t)$ is

$$P^{(3)}(t) = \alpha^{-1/2}\tilde{E}_0(\alpha t + \omega_0)\exp[i(\alpha t/2 + \omega_0)t] \times(2\pi)^{-1}\int_0^{\omega_0} d\Omega\tilde{\chi}^{(3)}(\Omega)\tilde{E}_s(\omega_0 - \Omega) \times\tilde{E}_0(\omega_0)\exp(i\Omega t). \quad (1)$$

As can be seen, one can multiply polarization $P^{(3)}(t)$ by the conjugate phase $\exp[-i(\alpha t/2+\omega_0)t]$ to remove the chirp of the pump that is mixed into the anti-Stokes signal. Because pump pulse spectrum $\tilde{E}_0(\omega)$ tends to be smooth, one can approximate it as a constant. Therefore one applies the inverse Fourier transform to $P^{(3)}(t)\exp[-i(\alpha t/2+\omega_0)t]$ to yield an estimate of the Raman spectrum $\tilde{\chi}^{(3)}(\Omega)$, weighted by the Stokes spectrum. Because the Stokes pulse spectrum tends to be slowly varying, this $\tilde{\chi}^{(3)}(\Omega)$ strongly resembles the true Raman spectrum.

To demonstrate this method, we acquired the complex Raman spectra of acetone, methanol, ethanol, and isopropanol. The system detailed in Fig. 2 was used. A 250 kHz repetition-rate regenerative amplifier (Regen amp) pulsed at 805 nm wavelength and 25 nm FWHM bandwidth. These pulses were split, with 90% of the light used to pump a second-harmonic-generation optical parametric amplifier (OPA). The remaining 10% was chirped to 6–10 ps by being passed through an 85 cm bar of BK7 optical glass, of which 45 mW was used as the CARS pump pulse. The OPA signal pulses were centered at 655 nm and 25 nm FWHM bandwidth, which were used to demodulate the anti-Stokes signal. The OPA idler pulses were centered at 1050 and 30 nm FWHM bandwidth, of which 2 mW served as the Stokes pulses.

A dichroic beam splitter combined the Stokes pulse to be coincident with the leading edge of the pump pulse. Both pulses were focused by a 30 mm focal-length achromatic lens into the sample liquid. The liquid partially filled a Petri dish with a gold mirror at the bottom to reflect the anti-Stokes light backward. A glass window was suspended over the Petri dish with one face dipped into the liquid to force the liquid surface to be flat and stationary, such that liquid motion would not produce changes in the interference. The reflected anti-Stokes light was separated by a dichroic beam splitter and overlapped the delayed reference pulse. A spectral interferogram corresponding to the real part of the Fourier transform of the temporal cross correlation between the pulses was sampled on the photodetector array. Resampling the interferogram to be linear in temporal frequency, setting the magnitude of the negative temporal frequencies to be zero, and using an inverse Fourier transform allowed the complex-analytic version of the temporal signal[11] to be recovered.

To calibrate the instrument, a nonresonant sample (sapphire) was used. Both the OPA signal and the anti-Stokes pulse are nearly transform limited and nearly identical. Therefore the angular dispersion of the wavelengths on the photodetector CCD array could be characterized. Then a sample of acetone was placed in the interferometer. Acetone has a strong, isolated resonance at 2925 cm^{-1}. Because of this single resonance, the anti-Stokes signal resembles the decaying, chirped sinusoid of Fig. 1(b). The dispersion introduced into the pump pulse by the BK7 bar was calibrated by adjusting the chirp dispersion parameter α. We optimized the value of by α by mini-

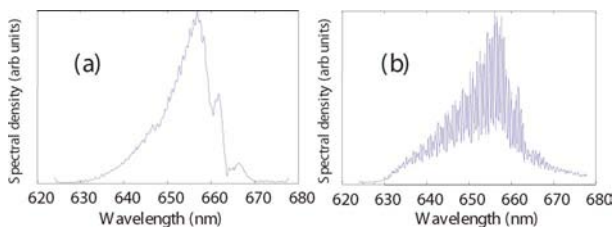

Fig. 3. (Color online) (a) Power spectrum of the anti-Stokes pulse from isopropanol. (b) Spectral interferogram of the anti-Stokes pulse.

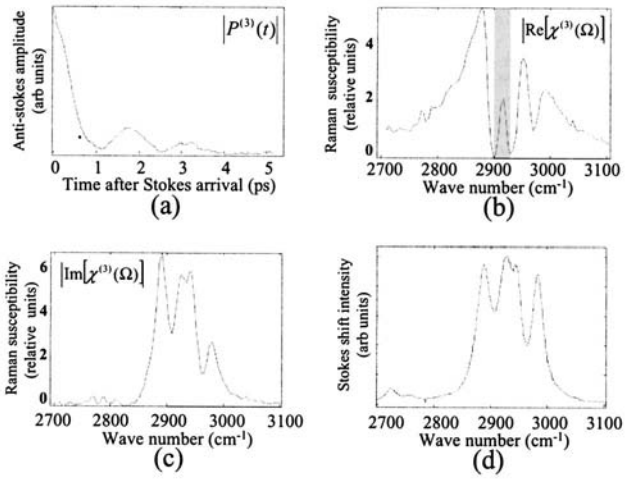

Fig. 4. (a) $|P^{(3)}(t)|$ of isopropanol. (b) $|\mathrm{Re}[\tilde{\chi}^{(3)}(\Omega)]|$. The shaded area corresponds to negative values of $\mathrm{Re}[\tilde{\chi}^{(3)}(\Omega)]$, which otherwise is positive. (c) $|\mathrm{Im}[\tilde{\chi}^{(3)}(\Omega)]|$. The sign of $\mathrm{Im}[\tilde{\chi}^{(3)}(\Omega)]$ is negative. The magnitude of the susceptibility is relative to (b). (d) The spontaneous Raman spectrum.

mizing the width of the computed spectrum and found α^{-1} to be 3.9×10^4 fs^2.

Finally, we experimentally demonstrate our method by measuring the Raman spectrum of isopropanol, which was chosen because the fine spectral detail tests the resolution of the instrument. Figure 3(a) shows the power spectrum of the anti-Stokes signal, which does not resemble the Raman spectrum, as expected for multiplex CARS. Figure 3(b) shows the spectral interferogram obtained for the anti-Stokes signal, from which the Raman spectrum was inferred. The primary noise source was photon noise, because the intensity of the spectrum was much greater than the thermally generated noise of the focal plane array. We sampled the spectrum by capturing 100 line scans gathered at a rate of 4000 Hz, so the total integration time was 25 ms.

Using the inverse Fourier transform, we converted this spectrum into the time-resolved anti-Stokes decay signal magnitude $|P^{(3)}(t)|$ of Fig. 4(a). The figure shows the envelope of the signal, including the beats between various Raman resonances. The inverse chirp was multiplied by the time-resolved decay signal, which was further Fourier transformed, resulting in the the Raman spectrum of Figs. 4(b) and 4(c). Figure 4(b) corresponds to $|\mathrm{Re}[\tilde{\chi}^{(3)}(\Omega)]|$, which includes the nonresonant component of the Raman susceptibility. Figure 4(c) corresponds to $|\mathrm{Im}[\tilde{\chi}^{(3)}(\Omega)]|$, which matches the spontaneous Raman spectrum given in Fig. 4(d), which was obtained by use of a commercial spectrometer. Because vibration caused subtle phase instability in the apparatus, we could not know the absolute phase of $\tilde{\chi}^{(3)}(\Omega)$, so we chose the value of $\tilde{\chi}^{(3)}(\Omega)$ at $\Omega=2800$ cm^{-1} as a reference for zero phase, because we knew *a priori* that the signal at this frequency is nonresonant. Furthermore, because of a slow drift in the relative delay between pump and Stokes beams, we could not determine instantaneous frequency ω_0 of the pump coincident with the arrival of the Stokes pulse. Therefore we could not calibrate the absolute frequency scale of the Raman spectrum. To aid in comparison, we have presented a scale that matches the known spectrum. Despite these limitations, it can be clearly seen that the spectral shape of $|\mathrm{Im}[\tilde{\chi}^{(3)}(\Omega)]|$ closely resembles the spontaneous Raman spectrum. Differences in peak heights are due to the Stokes pulse spectrum's being nonuniform over all Raman frequencies probed. As shown in Fig. 4(c), even the two peaks at 2928 and 2942 cm^{-1} can be clearly discerned by this method, even though the pump pulse is nearly 400 cm^{-1} in bandwidth. Similar correspondence between spectra acquired with our technique and from a commercial spectrometer were observed for acetone, methanol, and ethanol.

We have shown that, by computationally removing the chirp of the anti-Stokes pulse, one can obtain a high-resolution Raman spectrum with a broadband chirped pump pulse and a broadband Stokes pulse. In the future we shall endeavor to improve the accuracy of this Raman spectroscopy technique and extend it to simultaneously chirped pump and Stokes pulses, so that it can ultimately become a versatile and configurable Raman spectroscopy method.

We thank Jeremy Bredfeldt for his technical contributions to our laser system. This research was supported in part by the National Institutes of Health (grant 1 R01 EB001777 to S. A. Boppart). D. Marks's e-mail address is dmarks@vivc.edu.

References

1. M. D. Duncan, J. Reintjes, and T. J. Manuccia, Opt. Lett. **7**, 350 (1982).
2. A. Zumbusch, G. R. Holtom, and X. S. Xie, Phys. Rev. Lett. **82**, 4142 (1999).
3. G. W. H. Wurpel, J. M. Schins, and M. Muller, Opt. Lett. **27**, 1093 (2002).
4. C. Otto, A. Voroshilov, S. G. Kruglik, and J. Greve, J. Raman Spectrosc. **32**, 495 (2001).
5. D. L. Marks and S. A. Boppart, "Nonlinear interferometric vibrational imaging," Phys. Rev. Lett. **92**, 123905 (2004).
6. K. P. Knutsen, J. C. Johnson, A. E. Miller, P. B. Petersen, and R. J. Saykally, Chem. Phys. Lett. **387**, 436 (2004).
7. J.-X. Cheng, L. D. Book, and X. S. Xie, J. Phys. Chem. B **106**, 8493 (2002).
8. C. L. Evans, E. O. Potma, and X. S. Xie, Opt. Lett. **29**, 2923 (2004).
9. L. Lepetit, G. Cheriaux, and M. Joffre, J. Opt. Soc. Am. B **12**, 2467 (1995).
10. D. L. Marks, C. Vinegoni, J. S. Bredfeldt, and S. A. Boppart, Appl. Phys. Lett. **85**, 5787 (2004).
11. L. Mandel and E. Wolf, *Optical Coherence and Quantum Optics* (Cambridge U. Press, 1995).